RSC Advances

COMMUNICATION

View Article Online
View Journal | View Issue

Cite this: *RSC Adv.*, 2015, **5**, 95405

Received 23rd October 2015
Accepted 29th October 2015

DOI: 10.1039/c5ra22241a

www.rsc.org/advances

Structures and photoluminescence properties of Alq_3 1D materials prepared by an extremely facile solution method

Wanfeng Xie,[a] Hui Song,[a] Jihui Fan,[a] Feng Jiang,[a] Huimin Yuan,[a] Shiyu Zhang,[c] Zhixian Wei,[a] Zhiyong Pang*[a] and Shenghao Han*[ab]

Ultra-long crystalline Alq_3 1 dimensional (1D) materials were prepared by using an extremely facile solution approach without any surfactant, SDS, anti-solvent, or other reagents. The Alq_3 1D materials have smooth surfaces and pentagonal or hexagonal cross-sections. The length of the microrods have α-phase crystalline structures. The prepared Alq_3 samples exhibit excellent green-light photoluminescence (PL) performance. The growth mechanism of the Alq_3 1D structures were discussed. The limitation conditions of the Alq_3 microrods were also studied. In addition, the influence of the volume of $CHCl_3$ on the microrods was discussed. This controllable growth method can potentially be extended to other functional organic nanomaterials.

Introduction

Since the first efficient organic light-emitting diode (OLED) based on tris(8-hydroxyquinoline) aluminum (Alq_3) was reported by Tang and Van Slyke in 1987,[1] Alq_3 has been widely employed as an active material in OLEDs owing to its excellent electron-transporting ability and thermal stability.[2,3] After decades of intensive research and development, Alq_3 continues to be the workhorse in low-molecular weight materials for OLEDs, spin valves (SVs), organic field effect transistors (OFETs) and panel displays.[4–10] Very recently, Alq_3-based bluish green fluorescent composite nano-spheres were successfully synthesized, which can be used as paper sensors for nitro-aromatic explosive detection.[11]

In view of the potential applications in nano-optoelectronic devices and their novel properties such as quantum size effect, macroscopic quantum tunneling effect, surface effect and spin-related effects, the synthesis of Alq_3 micro/nanostructures, particularly one-dimensional (1D) crystals, attracted increasing research interesting in the last decades.[12–16] So far, the Alq_3 nanomaterials were mainly synthesized by vapor deposition-based or solution-based method.[17–24] Compared with the high temperature synthesis process of the vapor phase methods, the solution methods are facile and simple energy-saving route for the fabrication of high-quality Alq_3 nanostructures.[25] Moreover, the solution methods allow people to explore the optical and electronic properties of individual Alq_3 nanorods or nanowires.[18,25] In 2007, Hu *et al.* firstly reported a facile self-assemble growth route assisted by surfactant in solution to synthesize Alq_3 nanorods. The prepared nanorods had regular hexagonal geometry, good crystallinity, and good field-emission performance.[18] Wei *et al.* prepared Alq_3 nanorods by a facile microemulsion route assisted by surfactants such as cetyltrimethylammonium bromide (CTBA) and sodium dodecyl sulfate (SDS) and investigated the photoluminescence of isolated nanorods.[25] In 2010, Wong's group reported the fabrication of Alq_3 sub-microwires by a facile anti-solvent diffusion method and studied the field emission and waveguide properties of the sub-microwires.[20] In these experiments, surfactants, anti-solvents, or other reagents were added as assistants. It was believed to be impossible to obtain Alq_3 nanostructures by evaporating Alq_3 solution in air directly.[20]

In this paper, we adopt for the first time an extremely facile solution process to fabricate high quality Alq_3 1D crystals without using any surfactant, SDS, anti-solvent, H_2O or other reagents assistant. The Alq_3 1D crystals were prepared by volatilizing Alq_3 solution at room temperature directly. The prepared Alq_3 samples exhibit excellent green-light PL performance. Our method can potentially be extended to other functional organic nanomaterials.

Experimental

The Alq_3 nanostructures were fabricated by using an extremely facile solution method. Firstly, a certain amount of Alq_3 (purity:

[a]*School of Physics, State Key Laboratory of Crystal Materials, Shandong University, Jinan 250100, P. R. China. E-mail: hansh@sdu.edu.cn; pang@sdu.edu.cn; Fax: +86 531 88365435; Tel: +86 531 88365435*

[b]*School of Space Science and Physics, Shandong University, Weihai 264209, P. R. China*

[c]*School of Optoelectronics, Beijing Institute of Technology, Beijing 100081, P. R. China*

99.5%) powder and chloroform ($CHCl_3$) solvent were mixed to prepare Alq_3 solution. The $CHCl_3$ have many advantages compare to other organic solvents such as ethanol, DMF, CH_3CN, CH_2Cl_2 and toluene. It is a very good solvent for Alq_3 and polarity index is 4.4. Moreover, its boiling point is 61 °C, which is suitable for the room temperature self-assembly of organic nanostructures. In this experiment, 200 mg Alq_3 powder and 5 ml $CHCl_3$ were mixed to prepare Alq_3 solution. The Alq_3 solution was agitated by magnetic stirrer for 12 h till Alq_3 powder was fully dissolved (see Fig. 1A and B). Then, a little of the Alq_3 stock solution (about 2 ml) was dropped onto the tilted polished Si substrates in a beaker by a long capillary needle. The Si substrates were previously cleaned by sequential ultrasonic rinses in acetone, ethanol, and deionized water. The beaker was sealed with parafilm to prevent the $CHCl_3$ from volatilizing quickly due to its relatively low boiling point. As the chloroform solvent volatilized off thoroughly, crystalline Alq_3 nanostructures were obtained. The whole processes were finished in a cabinet with exhaust device to avoid volatilizing Alq_3 solution in air directly, finally the volatized $CHCl_3$ and byproduct ($COCl_2$) can be dissolved in ethanol as possible by this method.

The microstructure analysis was carried out on a powder X-ray diffractometer (PXRD, Bruker AXS, D8 Advance). The surface morphology and element analysis of the samples were characterized by a high resolution scanning electron microscope (SEM, S-4800) and a transmission electron microscope (TEM, Tecnai G^2 F20) in combination with energy dispersive X-ray (EDX). Fourier transform infrared spectroscopy (FTIR) pattern was studied by using FT-IR spectrophotometer (Thermo Nicolet, NEXUS 670). The PL signal from the sample was dispersed by a Jobin-Yvon iHR320 monochromator excited at 325 nm and detected by a thermoelectrical cooled Synapse CCD detector at room temperature.

Results and discussion

Fig. 2 shows the SEM images of the as-prepared Alq_3 samples. Randomly distributed Alq_3 1D materials with smooth surfaces along with their entire length can be clearly seen when the concentration of Alq_3 solution is 40 mg ml^{-1}. Three kinds of Alq_3 1D materials, rod-shaped microstructures with irregular pentagonal (Fig. 2A), quadrilateral (Fig. 2A), or hexagonal

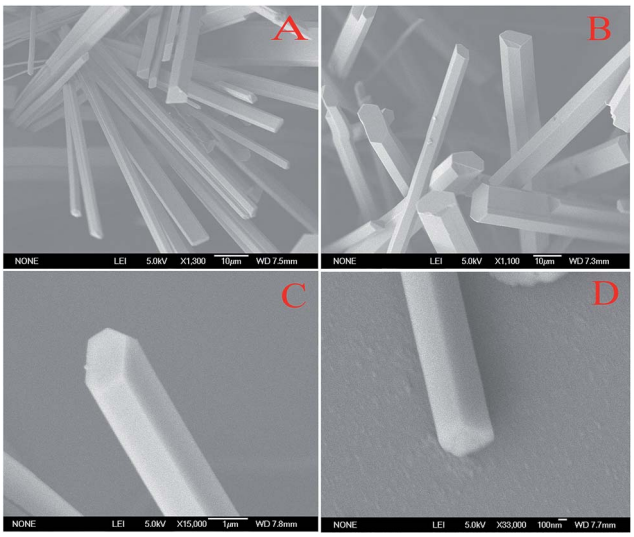

Fig. 2 The SEM photographs of the as-prepared Alq_3 1D structures. (A) Rod-shaped microstructures with irregular pentagonal or quadrilateral cross-sections. (B) Microrods with regular or irregular hexagonal cross-sections. (C) and (D) Nanorods with regular quadrilateral and hexagonal cross-sections, respectively.

(Fig. 2B) cross-section ones could be observed. The length of the longest rod can reach ~100 μm with an aspect ratio of length/diameter (L/D ratio) of about 12. It is necessary to point out that the density of the Alq_3 microrods can be possibly controlled by growth environment, such as the concentration of Alq_3 solution and the volatilization speed of the $CHCl_3$.[25] In particular, other nanostructures instead of microrods will be obtained as the concentration of the Alq_3 solution insufficient. For example, rice-like nanoparticles will be fabricated when the concentration of Alq_3 solution is about 7–13 mg ml^{-1}.[26] A main reason is that the concentration of the Alq_3 solution directly affects the growth time of Alq_3 crystals (nuclei). The different growth time of the Alq_3 nuclei leads to different shapes and sizes of the particles.

Fig. 3 shows a TEM image and the corresponding energy dispersive X-ray (EDX) of the prepared microrods. The TEM image confirms further that the prepared samples are solid rods. Few defects can be observed from the Alq_3 microrods (Fig. 3A). The result of EDX microanalysis proves the C, N, O

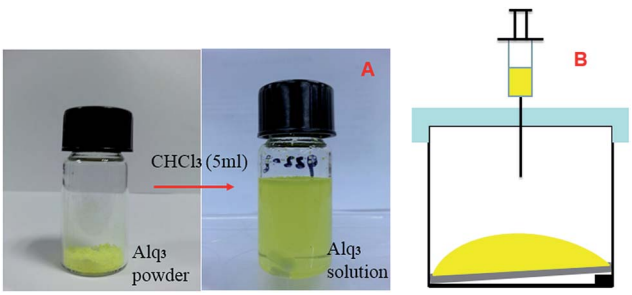

Fig. 1 A schematic view of the preparation process of the Alq_3 solution and crystalline Alq_3 nanostructures. (A) The Alq_3 solution preparation process, and (B) the growth process of Alq_3 microrods.

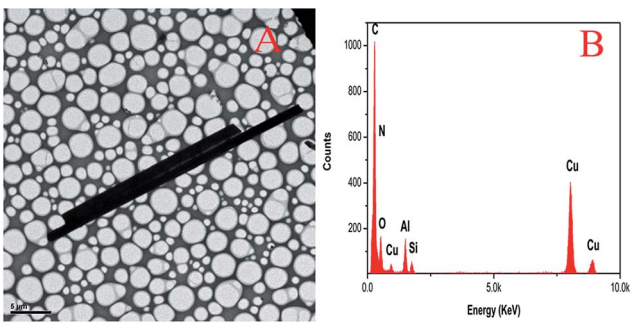

Fig. 3 (A) TEM image and (B) EDX element analysis of Alq_3 microrods.

and Al chemical composition of the prepared Alq_3 microrods (Fig. 3B). Because the samples for TEM and EDX were scraped from the Si substrates and transferred onto Cu grids coated with carbon films, peaks of Cu and Si elements were also observed.

The FTIR and PXRD spectra were recorded to reveal the composition and microstructure of the obtained Alq_3 microrods. The FTIR spectrum was measured in the range of 400–1000 cm^{-1} (see Fig. 4A). The peaks at 522.62, 548.09, and 749.20 cm^{-1} belong to the stretching vibrations of Al–O, and the peak at 419.53 cm^{-1} is assigned to the Al–N stretching vibrations of α-phase Alq_3.[18] The PXRD pattern in Fig. 4B matches well with that of the α-phase Alq_3 1D structures,[14,17–19,22] confirming further that the prepared microrods are α-phase Alq_3 with a preferred orientation of [001] direction, that is, the crystallographic *c*-axis direction.[19] For reference, the FTIR and PXRD of Alq_3 powder were also measured as shown in Fig. 4C and D, respectively.

According to the above analysis, we tentatively give a possible growth mechanism of Alq_3 microrods fabricated by volatilizing Alq_3 solution and the sketch map was illustrated in the Fig. 5. At the first step, Alq_3 solution was injected onto the Si substrates and form one large droplet, then the chloroform ($CHCl_3$) begin to volatilize from the Alq_3 stock solution at room temperature attributing to its relatively low boiling point. Gradually, the concentration of the droplet increases slowly and supersaturates that leads to nucleation.[25] Solvent evaporation during crystal seeds formation results in extensive phase separation. Simultaneously, the position of many Alq_3 molecules can transfer toward to the nuclear seeds then formed nanoparticles. This produces relatively large Alq_3 molecules rich domains between nanoparticle aggregates within the nanorods. Eventually, theses Alq_3 nanoparticles grow into crystalline rods along the crystallographic *c*-axis direction under the forces of van der

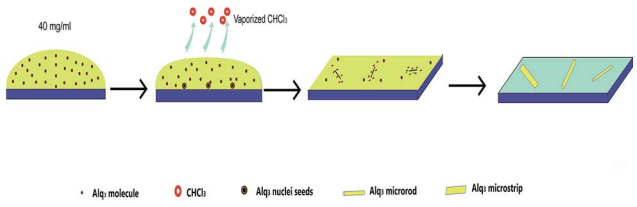

Fig. 5 Sketch of the growth mechanism of Alq_3 microrods.

Waals, Coulomb interaction of the anionic π electrons of the quinoline rings of Alq_3 molecules.[17,25,27] In addition, the hydrogen bonding in organic solvent ($CHCl_3$) play an very important role in the formation of the Alq_3 microrods in liquid phase.[28] For example, Whitesides's group reported that the self-assembly of bisCA (1,2,3) and bisM (5,6) forms nanorod materials [(bisCA)*n*(bisM)*n*] in organic solvents such as $CHCl_3$ and that these rods aggregate into mesoscopic aggregates of rod.[29] In fact, the migration of Alq_3 molecules are involved in the whole self-assembly process during the formation of the Alq_3 rods. However, the detailed kinetic process of Alq_3 molecules need further investigation.

Fig. 6 shows the temperature-dependent (50 K, 100 K, 150 K, 200 K, 250 K and 300 K) PL spectra of the Alq_3 microrods. The peaks show a good symmetry in the range of 400 nm to 700 nm, which has an obvious difference with that of the ε-phase Alq_3 fabricated by the physical vapor deposition (PVD) method.[30] One possible reason might be the difference in crystalline phase and the crystal size. Also, all spectra are similar in shape with one broad band. As a molecule is excited from S_0, the electron remains correlated with the hole left behind.[31] The electrons and holes will be located either in a molecule or different neighboring molecules. The abundant intrinsic molecular electronic states, together with the interaction of intermolecules, result in a large number of energy levels in the Alq_3 rods, which give birth to broad emission bands.[30,31]

Moreover, the PL intensity and peak position are slightly dependent on the temperatures. Generally, the PL intensity decreases greatly with the temperature increases from 50 K to 300 K, that is the emission intensity at low temperature is stronger than that of high temperature attributed to the weak coupling of photons and phonons at low temperature.[26] The

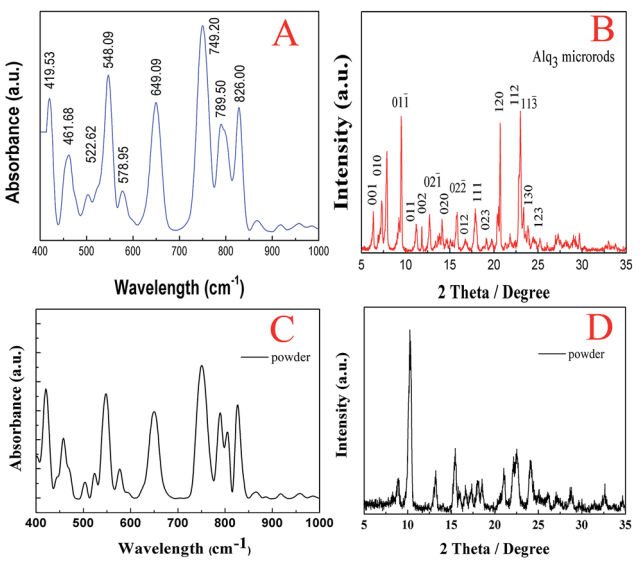

Fig. 4 (A) The FTIR pattern of the α-Alq_3 microrods. (B) PXRD pattern of sample of Alq_3 microrods. (C) The FTIR spectrum of Alq_3 powder. (D) PXRD pattern of Alq_3 powder.

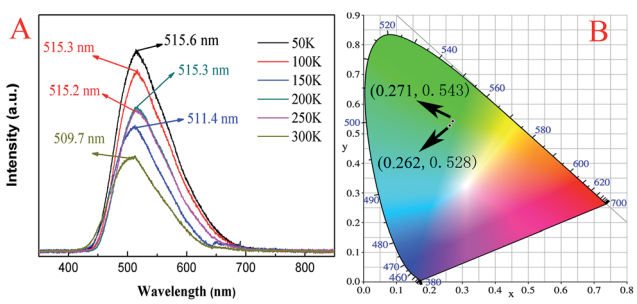

Fig. 6 (A) Temperature-dependent PL spectra of Alq_3 microrods excited at 325 nm. (B) The calculated CIE chromaticity coordinates (0.271, 0.543) at 50 K and (0.262, 0.528) at 300 K of the Alq_3 microrods.

area ratio of PL spectra at room temperature and the maximum at low temperature, which is defined as internal quantum efficiency (IQE) in some paper, are calculated to be 47.7% of the sample.[30] The peak positions reveal an evident blue shift (about 6 nm) with the increase of the temperature. For example, the peak position is 509.7 nm at 300 K and 515.6 nm at 50 K, as shown in the Fig. 6A. The blue shift in PL energies with increasing temperature has been observed in other organic semiconductors such as PHP,[32] MeLPPP,[32] PPV and MEH-PPV,[33,34] which have typically been attributed to lattice fluctuations. The shift in electronic energies reflect on the temperature dependence of the actual relaxation process whereby the exciton remains more localized on smaller chain segments on increasing the temperature.[32]

The spectra exhibit a very strong light emission with its maximum peak position at 515.6 nm at 50 K which corresponds to the radiative recombination of singlet excitons $S_1 \rightarrow S_0$ in *mer*-Alq_3.[33,34] The CIE chromaticity coordinates of the PL spectra have been calculated by using software CIE1931. The calculated CIE coordinates of the PL spectra at 50 K and 300 K are (0.271, 0.543) and (0.262, 0.528), respectively (see Fig. 6B), which are typical green emissions.[35,36]

Conclusions

In summary, we demonstrate a new one-step solution process for the controlled growth of 1D structured Alq_3. The Alq_3 microrods were fabricated by volatilizing Alq_3 solution directly at room temperature. No surfactant, SDS, anti-solvent, H_2O or other reagents assistant was used in our experiment. PXRD and FTIR spectra suggest that the fabricated Alq_3 1D microrods have α-phase crystalline microstructures. The PL spectrum of the microrods exhibits a very strong peak at 515 nm with a symmetric curve in the range of 450 nm to 650 nm. Our method also could be extended to other functional organic materials.

Acknowledgements

The authors are grateful for financial support from the Natural Science Foundation of China (61176019, 11374184, 11444007, and 61106083).

Notes and references

1 C. W. Tang and S. A. VanSlyke, *Appl. Phys. Lett.*, 1987, **51**, 913–915.
2 S. J. Fang, Z. Y. Pang, L. Lin, F. G. Wang, W. F. Zheng, Y. H. Li, Y. Dai and S. H. Han, *Phys. E*, 2011, **43**, 1470–1474.
3 M. Muccini, M. A. Loi, K. Kenevey, R. Zamboni, N. Masciocchi and A. Sironi, *Adv. Mater.*, 2004, **16**, 861–864.
4 M. Brinkmann, G. Gadret, M. Muccini, C. Taliani, N. Masciocchi and A. Sironi, *J. Am. Chem. Soc.*, 2000, **122**, 5147–5157.
5 D. L. Sun, L. F. Yin, C. J. Sun, H. W. Guo, Z. Gai, X. G. Zhang, T. Z. Ward, Z. H. Cheng and J. Shen, *Phys. Rev. Lett.*, 2010, **104**, 236602.
6 B. Yu, L. Z. Huang, H. B. Wang and D. H. Yan, *Adv. Mater.*, 2010, **22**, 1017–1020.
7 S. J. Zhang, N. J. Rolfe, P. Desai, P. Shakya, A. J. Drew, T. Kreouzis and W. P. Gillin, *Phys. Rev. B: Condens. Matter Mater. Phys.*, 2012, **86**, 075206.
8 A. Mishra, N. Periasamy, M. P. Patankar and K. L. Narasimhan, *Dyes Pigm.*, 2005, **66**, 89–97.
9 S. N. Al-Busafi, F. O. Suliman and Z. R. Al-Alawi, *Dyes Pigm.*, 2014, **103**, 138–144.
10 K. P. Dhakal, H. Lee and J. Y. Kim, *Synth. Met.*, 2014, **190**, 44–47.
11 Y. X. Ma, H. Li, S. Peng and L. Y. Wang, *Anal. Chem.*, 2012, **84**, 8415–8421.
12 S. J. Zhang, T. Kreouzis and W. P. Gillin, *Synth. Met.*, 2013, **173**, 46–50.
13 W. P. Gillin, S. J. Zhang, N. J. Rolfe, P. Desai, P. Shakya, A. J. Drew and T. Kreouzis, *Phys. Rev. B: Condens. Matter Mater. Phys.*, 2010, **82**, 195208.
14 T. Fukushima and H. Kaji, *Org. Electron.*, 2012, **13**, 2985–2990.
15 H. Bi, H. Y. Zhang, Y. Zhang, H. Z. Gao, Z. M. Su and Y. Wang, *Adv. Mater.*, 2010, **22**, 1631–1634.
16 C. P. Peter, L. W. Kennet and M. J. Brett, *Adv. Mater.*, 2006, **18**, 224–228.
17 C. P. Cho, C. A. Wu and T. P. Perng, *Adv. Funct. Mater.*, 2006, **16**, 819–823.
18 J. S. Hu, H. X. Ji, A. M. Cao, Z. X. Huang, Y. Zhang, L. J. Wan, A. D. Xia, D. P. Yu, X. M. Meng and S. T. Lee, *Chem. Commun.*, 2007, 3083–3085.
19 A. M. Collins, S. N. Olof, J. M. Mitchels and S. Mann, *J. Mater. Chem.*, 2009, **19**, 3950–3954.
20 G. Xu, Y. B. Tang, C. H. Tsang, J. A. Zapien, C. S. Lee and N. B. Wong, *J. Mater. Chem.*, 2010, **20**, 3006–3010.
21 D. J. Jan, S. S. Wang, S. J. Tang, K. Y. Lin, J. J. Yang and J. L. Shen, *Thin Solid Films*, 2011, **520**, 1005–1009.
22 M. Cölle and W. Brütting, *Phys. Status Solidi A*, 2004, **201**, 1095–1114.
23 M. Rajeswaran and T. N. Blanton, *J. Chem. Crystallogr.*, 2005, **35**, 71–76.
24 M. Braun, J. Gmeiner, M. Tzolov, M. Coelle, F. D. Meyer, W. Milius, H. Hillebrecht, O. Wendland, J. U. von Schütz and W. Brütting, *J. Chem. Phys.*, 2001, **114**, 9625–9632.
25 W. Chen, Q. Peng and Y. D. Li, *Adv. Mater.*, 2008, **20**, 2747–2750.
26 W. F. Xie, J. H. Fan, H. Song, F. Jiang, H. M. Yuan, Z. X. Wei, Z. W. Ji, Z. Y. Pang and S. H. Han, *Chem. Commun.*, 2015, 004228.
27 M. Cölle, C. Gärditz and M. Braun, *J. Appl. Phys.*, 2004, **96**, 6133–6141.
28 A. Nangia and G. R. Desiraju, *Chem. Commun.*, 1999, 605–606.
29 I. S. Choi, X. H. Li, E. E. Simanek, R. Akaba and G. M. Whitesides, *Chem. Mater.*, 1999, **11**, 684–690.
30 W. F. Xie, Z. Y. Pang, Y. Zhao, F. Jiang, H. M. Yuan, H. Song and S. H. Han, *J. Cryst. Growth*, 2014, **404**, 164–167.
31 G. Y. Zhong, X. M. Ding, J. Zhou, N. Jiang, W. Huang and X. Y. Hou, *Chem. Phys. Lett.*, 2006, **420**, 347–353.

32 S. Guha, J. D. Rice, Y. T. Yau, C. M. Martin, M. Chandrasekhar, H. R. Chandrasekhar, R. Guentner, P. Scanduicci de Freitas and U. Scherf, *Phys. Rev. B: Condens. Matter Mater. Phys.*, 2003, **67**, 125204–125211.
33 S. H. Lim, T. G. Bjorklund and C. J. Bardeen, *Chem. Phys. Lett.*, 2001, **342**, 555–562.
34 T. W. Hagler, K. Pakbaz, K. F. Voss and A. J. Heeger, *Phys. Rev. B: Condens. Matter Mater. Phys.*, 1991, **44**, 8652–8666.
35 R. J. Curry and W. P. Gillin, *J. Appl. Phys.*, 2000, **88**, 781–785.
36 M. Cölle and C. Gärditz, *Appl. Phys. Lett.*, 2004, **84**, 3160–3162.